JOURNAL OF Materials CHEMISTRY

Synthesis and crystal engineering of new halogenated tetrathiafulvalene (TTF) derivatives and their charge transfer complexes and radical ion salts†

Andrei S. Batsanov,[a] Martin R. Bryce,*[a] Antony Chesney,[a] Judith A. K. Howard,[a] Derek E. John,[a] Adrian J. Moore,[a] Clare L. Wood,[a] Hagit Gershtenman,[b] James Y. Becker,*[b] Vladimir Y. Khodorkovsky,*[b] Arkady Ellern,[b] Joel Bernstein,[b] Igor F. Perepichka,[c] Vincent Rotello,[d] Mark Gray[d] and Alejandro O. Cuello[d]

[a]*Department of Chemistry, University of Durham, Durham, UK DH1 3LE. E-mail: m.r.bryce@durham.ac.uk*
[b]*Department of Chemistry, Ben-Gurion University of the Negev, Beer-Sheva, 84105, Israel*
[c]*L. M. Litvinenko Institute of Physical Organic & Coal Chemistry, National Academy of Sciences of Ukraine, Donetsk, 83114, Ukraine*
[d]*Department of Chemistry, University of Massachusetts at Amherst, Amherst, MA 01003, USA*

Received 27th February 2001, Accepted 22nd May 2001
First published as an Advance Article on the web 11th July 2001

Efficient syntheses are reported for tetraiodotetrathiafulvalene **2**, 4-iodo-5-methyl-4′,5′-bis(methylsulfanyl)TTF **3**, and 4-iodo-4′,5′-bis(methylsulfanyl)TTF **4** by iodination, using perfluorohexyl iodide, of lithiated derivatives of the corresponding TTF system. Bromination and chlorination of lithiotrimethylTTF using 1,2-dibromotetrafluoroethane and hexachloroethane gave 4-bromo- and 4-chloro-4′,5,5′-trimethylTTF **6** and **7**, respectively. Phosphite-induced self-coupling or cross-coupling reactions of 4-iodo-1,3-dithiole-2-thione or 4,5-diiodo-1,3-dithiole-2-thione(one) half-units resulted in TTF derivatives with partial loss of the iodine substituent(s). 4,5-Dibromo-4′,5′-bis(cyanoethylsulfanyl)TTF **15** was prepared by cross-coupling methodology, and converted into 4,5-dibromo-4′,5′-bis(methylsulfanyl)TTF **16** by reaction with caesium hydroxide and then methyl iodide. EPR data are reported for the electrochemically generated cation radicals of trimethylTTFX derivatives (X = I, Br and Cl) **5–7**, respectively. For the neutral donors, the X-ray crystal structures are reported for **2**, **5**, **6**, tetramethylTTF **8** and **15**. Structure **2** is characterised by a particularly dense packing with continuous chains of intra-stack I···I contacts (4.17–4.19 Å). The crystals of **6** and **8** are isomorphous, while the structure of **5** is different. The iodo-substituent in **5** affects the packing in a way the bromo-substituent in **6** does not, due to differences in specific interactions rather than steric demands of I and Br, which are similar. Structure **15** comprises face-to-face dimers with inter-dimer Br···Br (3.57 Å) and Br···S (3.55 Å) contacts: a remarkable difference in bond distances between the Br and S-substituted dithiole rings is observed. The 1 : 1 charge-transfer (CT) complexes **3**·TCNQ and **4**·TCNQ (TCNQ = 7,7,8,8-tetracyano-*p*-quinodimethane, **17**) display mixed stair-like stacks of alternating D and A moieties: the overall degree of CT is estimated from bond length analysis to be 0.2 *e* and 0.3 *e*, respectively. In **3**·TCNQ either position of the disordered iodine atom has one short (inter-stack, but intra-layer) contact with a cyano group (I···N distances of 3.14 and 3.18 Å). In **4**·TCNQ a similar I···N contact is much longer (3.35 Å). In the structure of $\mathbf{5}^{+\cdot}\mathrm{I_3}^{-}\cdot\frac{1}{2}\mathrm{I_2}$ the cation radical is disordered; dimeric cation radicals display short intra-dimer contacts (S···S 3.38–3.39 Å, C···C 3.35 Å) consistent with electron coupling. Each dimer is surrounded by four $\mathrm{I_3}^{-}$ anions. The crystal structure of $\mathbf{16}^{+\cdot}\mathrm{I_3}^{-}$ is comprised of layers with interplanar separations of 3.55 Å. Cations of one layer overlap with anions of the next, and the packing can be described as mixed stacks parallel to the *a* axis. The remarkably high conductivity of this salt for a system of 1 : 1 stoichiometry ($\sigma_{rt} = 8 \times 10^{-2}$ S cm^{-1}) is ascribed to partial charge transfer (the charge on the TTF moiety is estimated as $+\frac{2}{3}$ from bond length analysis) and a continuous system of short non-bonding contacts.

Introduction

Within the field of molecular conductors,[1] crystal engineering[2] has emerged as a key topic.[3] Tetrathiafulvalene (TTF) and its derivatives are electron donors *par excellence* for the formation of charge-transfer complexes and radical ion salts[4] due to the planarity (or near-planarity) and high chemical stability of a radical cation[5] which favour the intermolecular delocalisation of charge carriers.[6] The formation of stacks of TTF cation radicals in the crystal lattice, with short interplanar distances, means that many salts are highly anisotropic (one-dimensional) materials.[1,6]

Close interstack sulfur···sulfur contacts increase the dimensionality in TTF derivatives,[1] although intermolecular hydrogen bonding,[1c,7] and interactions involving halogen atoms[8] have gained increasing attention in this context. The attachment of halogen atoms to TTF[8,9] reduces the π-electron donating ability and this effect is additive with an increasing

†Electronic supplementary information (ESI) available: a table of intermolecular contacts for compounds **2**, **5**, **6**, **8**, **15**, **3**·TCNQ, **4**·TCNQ, **1**·**18**, **1**·**19**·2$C_4H_8O_2$, $\mathbf{5}^{+\cdot}\mathrm{I_3}^{-}\cdot\mathrm{I_2}$ and $\mathbf{16}^{+\cdot}\mathrm{I_3}^{-}$, and a figure of the crystal structure of complex **1**·**18**. See http://www.rsc.org/suppdata/jm/b1/b101866n/

number of halogens on the TTF system.[8a] We reported that the crystal structures of two cation radical salts of 4-iodoTTF **1** are characterised by short intermolecular contacts involving the iodine substituent.[10] The key motivation behind the present work was the study of new iodinated- and brominated-TTF derivatives with the aim of elucidating the role played by the halogen atoms in modifying the solid state structures of the neutral species and their charge transfer complexes and radical ion salts.

Results and discussion

Synthesis

The usual routes to functionalised TTFs comprise: (a) reactions of lithiated TTF species with electrophiles,[11] and (b) coupling (or cross-coupling) of two 1,3-dithiole-2-thione (or ketone) half-units, usually in the presence of trialkyl phosphite.[12] We have explored both of these methods for the synthesis of iodinated- and brominated-TTFs.

Between 1989 and 1994 three groups independently reported the failure to obtain tetraiodoTTF **2** by direct lithiation/iodination of TTF using either iodine, tosyl iodide or perfluorohexyl iodide as the iodinating reagent.[9] In 1995 Gompper *et al.* published a synthesis of **2** by a different route, *viz.* the self-coupling of 4,5-diiodo-1,3-dithiole-2-one **9** (triethyl phosphite, toluene, 110 °C, 68% yield) along with the X-ray crystal structure of the salt $I_4TTF^{+\cdot}\cdot I^-$.[13] However, we found that coupling of compound **9**, or the thione analogue **10**, in the presence of triethyl phosphite under a variety of conditions, including those reported by Gompper *et al.*,[13] did not proceed as stated. Instead, a complex product mixture was repeatedly obtained, comprising mono-, di- and tri-iodoTTF, with only a small amount (<10%) of tetraiodoTTF **2** present (mass spectrometric and TLC evidence). Clearly, in our hands, extensive deiodination was accompanying the coupling reaction. While our work was in progress, Sato and Sensui published a low-yielding synthesis of **2** [26% yield, after separation from 4,4′(5′)-diiodoTTF] by sequential reaction of TTF with LDA (10 equivalents) and iodine (10 equivalents).[14] We now report that compound **2** can be obtained in 84% yield under precisely-controlled conditions by lithiation of TTF (8 equivalents of LDA in THF) followed by the addition of perfluorohexyl iodide[8a,15] (8 equivalents) at −50 °C. Compound **2**, which is insoluble in most organic solvents, was isolated as red needles with mp 203 °C (decomp.) [*cf.* mp 196–202 °C (decomp.) reported by Sato and Sensui[14] and a very different mp of 175 °C (decomp.) claimed for **2** by Gompper *et al.*[13]] We have unambiguously established the structure of I_4TTF **2** by single crystal X-ray analysis (see below).

We have found that cross-coupling is also not a good method for the preparation of mono- or di-iodoTTFs. For example, reactions of 4-iodo-1,3-dithiole-2-thione[16] or diiodo analogues **9**[13] and **10**[13] with **11**[17] [neat $P(OEt)_3$ at 100 °C or reflux, or $P(OEt)_3$ in refluxing toluene] always led to mixtures of TTF derivatives which had suffered a significant loss of iodine (^1H NMR, mass spectrometric and TLC evidence — no coupling occurred at lower temperatures). Comparable deiodination

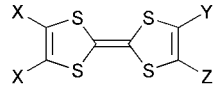

	X	Y	Z
1	H	H	I
2	I	I	I
3	SMe	Me	I
4	SMe	H	I
5	Me	Me	I
6	Me	Me	Br
7	Me	Me	Cl
8	Me	Me	Me

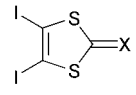

9 X = O
10 X = S

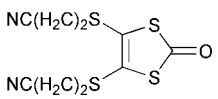

11

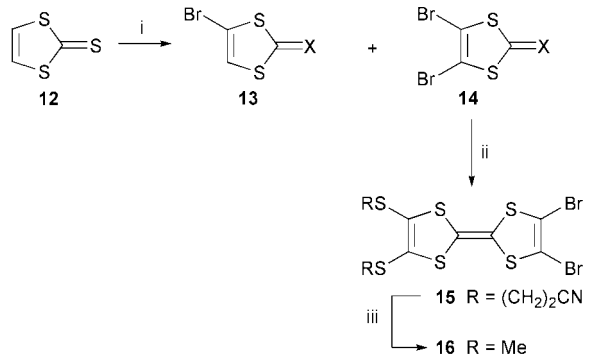

12 **13** **14** **15** R = $(CH_2)_2CN$ **16** R = Me

Scheme 1 *Reagents and conditions*: LDA, ether, −78 °C, then toluene-*p*-sulfonyl bromide, −78 °C to −20 °C; ii compound **11**, $P(OEt)_3$, toluene, reflux; iii $CsOH\cdot H_2O$, THF–methanol, 20 °C, then MeI, 20 °C.

reactions in other cross-couplings have been noted by Imakubo *et al.*,[16] but Garín *et al.* do not mention deiodination in the cross-coupling of **9** with 4,5-dicarbomethoxy-1,3-dithiole-2-one [using $P(OMe)_3$] although no temperature or yield were reported for this reaction).[18]

It is apparent that the iodination of a preformed TTF derivative is the most reliable method of synthesising iodoTTFs. This protocol has yielded compounds **1**[10] and **5**[19] and we now describe the new analogues **3** and **4**. Lithiation of 4-methyl-4′5′-bis(methylsulfanyl)TTF and 4,5-bis(methylsulfanyl)TTF followed by reaction with perfluorohexyl iodide led to the clean formation of products **3** and **4**, in 65% and 40% yields, respectively.

We next turned to the synthesis of new brominated TTF derivatives. Lithiation of vinylene trithiocarbonate **12** followed by reaction with toluene-*p*-sulfonyl bromide or 1,2-dibromotetrafluoroethane gave a mixture of mono- and di-bromo derivatives, **13** and **14**, respectively, which were readily separated by chromatography (Scheme 1). Cross-coupling of **11** with **14** gave TTF derivative **15** (38% yield) with no loss of bromine (*cf.* the extensive loss of iodine when **9** or **10** were used in this reaction, as discussed above). Removal of the cyanoethyl groups of **15** under Becher's conditions (caesium hydroxide in methanol)[20] generated the dithiolate species which was trapped *in situ* with iodomethane to afford **16**, which had previously been synthesised from 4,5-bis(methylsulfanyl)TTF.[8d] Similarly, bromination (using 1,2-dibromotetrafluoroethane) and chlorination (using hexachloroethane) of 4-lithiotrimethylTTF[21] gave compounds **6** and **7**, respectively.

Solution electrochemical data

The solution electrochemical data, obtained by cyclic voltammetry, for the haloTTF derivatives reported herein, along with model compounds for comparison, are collated in Table 1. Comparing compounds **5–7** with trimethylTTF the obvious trend resulting from halogen substitution is that both the first

Table 1 CV data for TTF derivatives[a]

Compound	$E_1^{\frac{1}{2}}$/mV	$E_2^{\frac{1}{2}}$/mV	ΔE
1	550	800	250
3	460	720	260
4	510	790	280
5	460	780	320
6	460	780	320
7	470	785	315
8	270	670	400
15	650	890	240
16	640	895	255
Me_3TTF	290	690	400

[a]Potentials are quoted *vs.* Ag/AgCl reference electrode. For details of conditions see the Experimental section. Reliable data could not be obtained for compound **2** due to insolubility.

Table 2 Experimental (and calculated) hyperfine coupling constants (r^2 for curve fitting >0.995) for **5–7**$^{+\cdot}$ [a]

Position	**5**$^{+\cdot}$	**6**$^{+\cdot}$	**7**$^{+\cdot}$
H_a	0.360	0.363	0.382 (0.536)
H_b	0.890	0.916	0.954 (0.823)
H_c	0.760	0.758	0.824 (0.805)

[a]Assignments are based on B3LYP/6-311G*//HF/3-21G*calculations for **7**$^{+\cdot}$ with averaging performed for the three hydrogens on each methyl group. Assignment of hfcs for methyl groups b and c are tentative.

and second oxidation potentials are raised significantly. The positive shift is the same (within experimental error) for I, Br and Cl. This was observed previously with TTF,[9b] but in contrast to this, for halogen substitution onto 4,5-dimethyl TTF the positive shift follows the sequence Cl > Br > I.[8a] It is notable for **5–7** that the value of $E_1^{\frac{1}{2}}$ is raised significantly more than $E_2^{\frac{1}{2}}$. As expected, the methyl substituent of compound **3** lowers the oxidation potentials compared to the unsubstituted analogue **4**. The methylsulfanyl substituents of **4** also slightly lower the first oxidation potential compared to the unsubstituted analogue **1**, a trend which has been noted previously when electron-withdrawing substituents (methoxycarbonyl) are present, although this is not always the case for methylsulfanyl substitution onto TTF.[22]

Simultaneous electrochemistry and EPR (SEEPR) spectra of 5–7

There are no reports on solution EPR spectra of halogenated TTF derivatives, so to probe further the structures of the species formed upon oxidation, halotrimethylTTF derivatives **5–7** were subjected to bulk electrolysis in dichloromethane solution to generate the cation radicals simultaneously with EPR signal acquisition. The data are presented in Table 2, and the experimental and simulated spectra of species **7**$^{+\cdot}$ are shown in Fig. 1. There are minor differences among the experimental hyperfine couplings in the SEEPR spectra. Direct assessment of these changes was hindered by the increased broadening observed with the bromo- and iodo-substituted derivatives, which are likely to be a consequence of the interaction between the unpaired electron spin on the TTF nucleus and the nuclear spin of the halogen.[23]

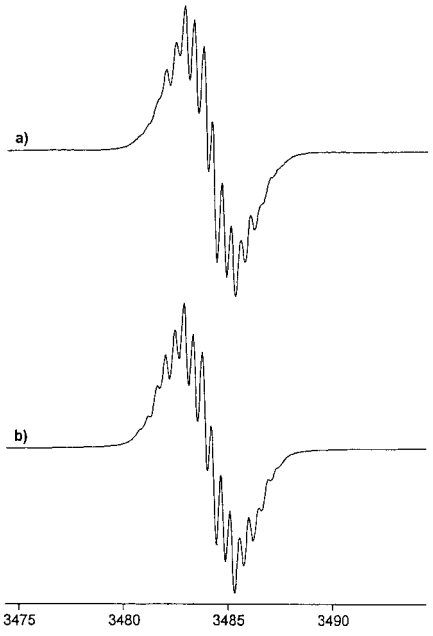

Fig. 1 Experimental (a) and simulated curve fit (b) SEEPR spectra for **7**$^{+\cdot}$.

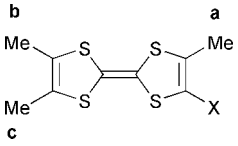

Chart 1

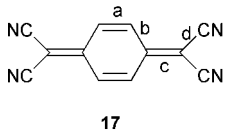

17

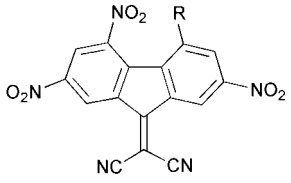

18 R = H
19 R = NO_2

Chart 2

Charge-transfer complexes: formation and electrical measurements

We successfully prepared several crystalline charge-transfer complexes of these halogenated-TTF donors, using TCNQ **17** and 9-dicyanomethylenefluorene derivatives **18** and **19** as electron acceptors (1 : 1 donor : acceptor stoichiometries) and the radical ion salts **5**$^{+\cdot}$$I_3^-$·$\frac{1}{2}I_2$ and **16**$^{+\cdot}$$I_3^-$ were prepared by diffusion of iodine vapour into solutions of the donor molecule. Their X-ray crystal structures are reported below. While our work was in progress the same salt **16**$^{+\cdot}$$I_3^-$ was obtained by Iyoda *et al.*, from electrocrystallisation experiments.[8d]

Complexes **3**·TCNQ and **4**·TCNQ and **1**·**18** have low electrical conductivity values, typical of mixed-stack systems ($\sigma_{rt} = 10^{-7}$–10^{-9} S cm^{-1}). The C≡N stretching frequencies in the IR spectra for **3**·TCNQ and **4**·TCNQ (2206 and 2204 cm^{-1}, respectively) suggest partial charge-transfer onto the TCNQ molecules.[24] A complex of **2** and F_4TCNQ (stoichiometry unknown) has a notably high compressed pellet conductivity ($\sigma_{rt} = 0.2$ S cm^{-1}, decreasing on lowering the temperature: *i.e.* typical semiconducting behaviour). The conductivity value for **5**$^{+\cdot}$$I_3^-$·$\frac{1}{2}I_2$ $\sigma_{rt} = 10^{-6}$ S cm^{-1} is typical of a 1 : 1 salt with complete charge transfer. The electrical properties of salt **16**$^{+\cdot}$$I_3^-$ are most unusual for a salt of this stoichiometry. Iyoda *et al.* reported a value of $\sigma_{rt} = 2.1 \times 10^{-2}$ S cm^{-1} for an electrocrystallised sample:[8d] the long needles of **16**$^{+\cdot}$$I_3^-$ we obtained have $\sigma_{rt} = 8 \times 10^{-2}$ S cm^{-1} (four-probe measurements) and from variable temperature data (300–80 K) the activation energy was found to be $E_a = 0.09$ eV which is typical of an organic semiconductor. Analysis of the crystal structure (see below) sheds light on this.

X-Ray crystal structures

Intermolecular interactions involving halogen atoms: general considerations. Introduction of halogen substituents into donor molecules can be an effective tool in crystal engineering of organic conductors and charge-transfer complexes. It has long been recognised[25] that halogen atoms (Cl, Br, and especially I) can form intermolecular donor–acceptor bonds with such donor atoms as O, N, Se, Te and with π-aromatic systems, the bond angle θ at the halogen atom, between covalent and donor–acceptor bonds, being close to 180°. The interaction of a donor atom D with a dihalogen molecule X–X can be almost as strong as a covalent bond, approaching the D$^+$–X···X$^-$ structure. The D···I–C interactions are much weaker, but are still considerably shorter than the sum of the van der Waals radii. There being no up-to-date review on this subject, we made a survey of N···I–C contacts, using the

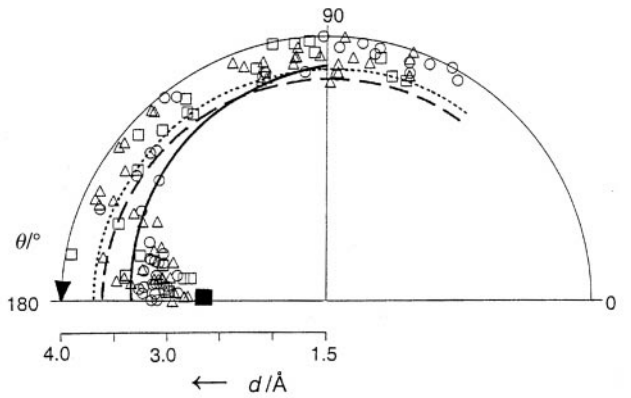

Fig. 2 Distribution of intermolecular N···I–C contacts by N···I distance d and N–I–C angle θ, for the nitrogen atoms participating in one (○), two (Δ) and three (□) covalent bonds (■ for the Ph–C≡C–I·morpholine complex[27]). The radial coordinate equals d–1.5 Å, *i.e.* represents the effective 'radius' of the iodine atom. Curves show the sums of van der Waals radii according to Rowland and Taylor[31] (···), Zefirov and Zorkii[30] (- - -), Nyburg and Faerman[33] (anisotropic model, –).

October 2000 release of the Cambridge Structural Database (CSD);[26] the results are presented in Fig. 2. For any state of hybridisation of the N atom, the largest number of contacts occur at θ angles close to 180°. For the linear N···I–C configuration, expected to be most favourable for donor–acceptor bonding,[25] the N···I distances are indeed considerably shorter than the 'normal' van der Waals contact, even taking into account the anisotropic shape of the iodine atom (*vide infra*). The angle between the N···I vector and the covalent bonds at the *nitrogen* atom show practically random overall distribution. However, the shortest contacts with sp^2 (aromatic) or sp^3 (pyramidal) N occur when its lone electron pair is pointing towards the iodine atom (no preferable orientation was obvious for cyano group N). Recently we re-examined the crystal structure[27] of the Ph–C≡C–I·morpholine complex, the formation of which is exothermic,[28] and found a linear N···I–C contact of 2.712(2) Å, more than 0.2 Å shorter than any observed before.

Crystals of halogen derivatives usually contain networks of intermolecular halogen···halogen contacts, often significantly shorter (by 0.1–0.4 Å) than the sums of the corresponding van der Waals radii and associated with certain preferable angular geometries.[29,30] These interactions can be regarded as a special case of donor–acceptor secondary bonding, the strength of which increases with the atomic polarisability (Cl < Br < I). Thus, I···I interactions stabilise the structure of 1,3,5,7-tetraiodoadamantane, while its Cl- and Br-analogues form plastic crystals.[29a] A histogram of *all* non-bonded Cl···Cl distances[31] (number of occurrences *vs.* the distance) from a survey of CSD has a distinct maximum at *ca.* 3.8 Å, while for most other elements such histograms show a monotonous increase with distance. This also reveals the tendency of halogen atoms to cohere in a crystal.

The most obvious way of elucidating specific interactions, a comparison of observed contacts with the sums of van der Waals radii, crucially depends on the correct choice of these radii, the widely used Bondi system[32] (1964) being rather obsolete. The atoms being neither absolutely 'hard' nor ideally spherical, the actual van der Waals contacts in crystals show a considerable range of distances, from which individual radii can be derived by two different approaches: a statistical analysis of *all* interatomic distances (some of which may not be direct contacts at all) or only of a limited number of 'structure-defining contacts' (the choice of which may be biased). Of the most up-to-date compilations, the former approach was adopted by Rowland and Taylor[31] and the latter by Zefirov and Zorkii,[30] whose systems give the lower and upper estimates, respectively (*viz.* 2.03 and 2.14 Å for iodine), hereinafter quoted as D_i. Both systems imply spherical atoms. However, a highly polarisable atom forming one covalent bond has a strongly anisotropic van der Waals shape which can be described by a rotational ellipsoid with the short axis collinear with the covalent bond and the long one normal to this bond (for iodine,[33] 1.76 *vs.* 2.13 Å). There is an ongoing controversy, whether the anisotropy is due to a reduction of van der Waals repulsion (the deformation of the 'real' atomic 'shape') or to specific attractive forces. A recent *ab initio* study confirmed the former view, by analysing the repulsion of probe He atoms, approaching from different directions.[34] On the other hand, molecular beam experiments have shown[29c] that the L-shaped geometry of the $(Cl_2)_2$ dimer implies specific attractive interaction. A statistical analysis of the CSD shows that the number of halogen–halogen contacts is larger than could be expected in proportion with the atom surface area.[29b] These and other experimental data (see above) also support the attraction model. The contact distances predicted by the anisotropic model[33] are quoted as D_a.

The electron accepting ability of a mono-coordinate halogen atom is maximum along the continuation of the covalent bond, but its electron donor ability is maximum in the perpendicular direction. Thus the shortened intermolecular contacts between two halogen atoms are consistent with attractive polarisation interactions or weak donor–acceptor bonding, when one atom has $\theta_1 \approx 180°$ and the other $\theta_2 \approx 90°$ (Chart 3, type *ii*). These interactions are structure-stabilising. The contacts with $\theta_1 \approx \theta_2$, *e.g.* where the contacting atoms are related *via* an inversion centre, are structurally irrelevant, 'space-filling' contacts, enforced by the overall requirements of crystal packing (Chart 3, type *i*).[29] The structures below are discussed in the light of these considerations. Intermolecular contacts are tabulated as supplementary data.†

Neutral donors 2, 5, 6, 8 and 15. The crystal structure of **2** contains two symmetrically non-equivalent molecules (A and B), both possessing crystallographic inversion centres (thus the asymmetric unit comprises two half-molecules). Both molecules are nearly planar with a small chair-like distortion, the dithiole rings folding by *ca.* 3.5° along the S···S vectors. Mean planes of molecules A and B form a dihedral angle of 55.5°, while the long axes of these molecules are nearly perpendicular (81°). Molecule B and its equivalents, related by the *a* translation, form an infinite stack with a longitudinal shift between adjacent molecules, so that the central C=C bond of one molecule overlaps with the dithiole ring of the next (Fig. 3). Molecules of type A form a different kind of stack, with a lateral shift between adjacent molecules (also related by the *a* translation). Here, an S atom of one molecule lies over the centre of the dithiole ring of the next. The interplanar separations in both stacks are uniform, 3.70 Å. Continuous chains of intra-stack I···I contacts (4.17–4.19 Å, *cf.* $D_a = 4.25$ Å) running parallel to the *a* axis, are space-filling (type *i*) contacts. On the contrary, the geometry of the interstack contacts I(2)···I(5) of 3.85 Å ($\theta = 87$ and 166°) and I(3)···I(6) of 3.99 Å ($\theta = 174$ and 101°) is consistent with an attractive interaction (see above), although the contacts are not particularly short ($D_a = 3.89$ Å). The interstack contact S(2)···I(6) of 3.54 Å is both substantially shorter than $D_a = 3.79$ Å and has a favourable geometry for attraction, forming an angle of 56° with the dithiole ring plane and

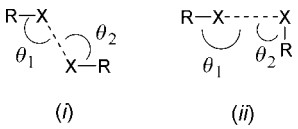

(*i*) (*ii*)

Chart 3

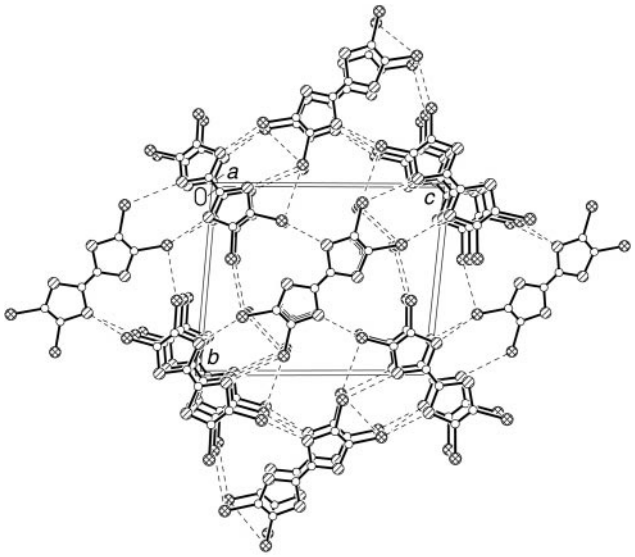

Fig. 3 Crystal structure of **2**, showing I···I contacts <4.3 Å and I···S contacts <4.0 Å. Primed atoms are generated by inversion centres.

$\theta = 163°$ at the I atom. A number of longer I···S contacts (3.73 to 3.99 Å) are inclined by 12–31° to the corresponding dithiole rings and have $\theta = 120$–$150°$, *i.e.* are less favourable. Generally, the crystal packing of **2** is particularly dense.

Comparison of **5**, **6** and **8** is instructive. Their molecular structures are similar, the TTF moieties folding along the S···S vectors by *ca.* 5° (**5**, **6**) or 6.5° (**8**) in a chair-like fashion. The crystal structure of **5** is monoclinic and chiral (space group $P2_1$), comprising stair-like stacks of molecules with a longitudinal slip between the adjacent molecules (Fig. 4). The interplanar separation of 3.76 Å is rather large, dictated by the bulky substituents. The molecule is disordered; the iodine substituent is distributed between four positions at C(2), C(3), C(5) and C(6) with the occupancies of 74, 4, 3 and 18%, respectively. Molecular planes in neighbouring stacks are nearly perpendicular. The C(2)–I(2) and C(6)–I(6) bonds of each molecule point towards the C(5)=C(6) and C(2)=C(3) bonds of the two molecules in adjacent stacks; the resulting I···C contacts of 3.36 to 3.43 Å (*cf.* $D_a = 3.68$ Å) may reflect a specific interaction, similar to Cl···π interactions, known to stabilise some host–guest complexes.[35]

In the triclinic crystal of **6** all molecules are parallel to the (102) plane and form a layered structure (Fig. 5) with an interlayer separation of 3.56 Å. The molecule has crystallographic C_i symmetry; the bromine substituent is disordered equally between all four positions (*i.e.* there is an overlap of 25% Br and 75% methyl in each). The shortest Br···S contacts, both intra-stack (3.77 Å) and inter-stack (3.85 Å) are not shortened ($D_i = 3.68$–3.81 Å). The packing mode of **8** is identical (Fig. 5) and the crystals of **6** and **8** are isomorphous. Thus the iodo-substituent in **5** affects the packing in the way the bromo-substituent in **6** does not. Similar disorder modes in **5** and **6** show that the steric demands of both I and Br do not differ significantly from that of methyl, hence the effect is due to specific interactions rather than the different size of I and Br atoms.

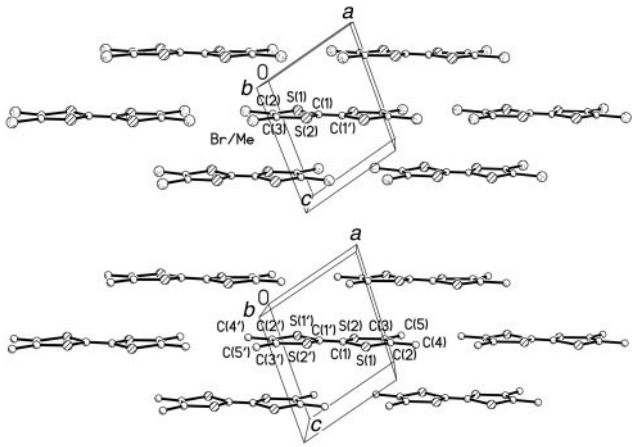

Fig. 5 Crystal structures of **6** (top) and **8** (bottom). H atoms are omitted.

Molecule **15** (Fig. 6) shows a small chair-like folding along the S(1)···S(2) and S(3)···S(4) vectors by 2.6 and 6.7°, respectively, and a remarkable difference of bond distances between the Br and S-substituted dithiole rings. This effect cannot be steric, the sizes of Br and S atoms being similar.[30–32] Neither can it be explained by stronger electron-withdrawing (σ-acceptor) ability of Br compared to S. The TTF HOMO has nodes on C–S but not on C=C bonds, hence electron withdrawal should result in shortening of all the C–S bonds and lengthening of the C=C bonds.[22b,c] Such a change has been observed on oxidation of a range of TTF systems.[36] In **15**, the S(3)–C(5), S(4)–C(6) and C(5)–C(6) bonds in the S-substituted ring are significantly longer (1.765(2), 1.764(2) and 1.351(3) Å)

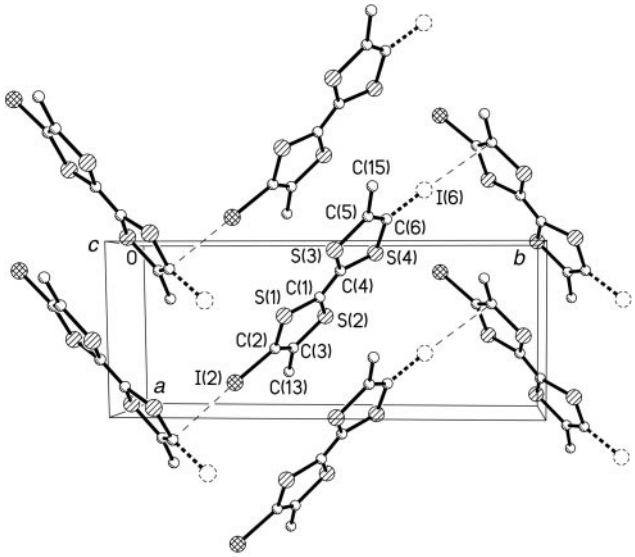

Fig. 4 Crystal structure of **5**, showing major positions of the disordered iodine atom, I(2) and I(6) (occupancies 74 and 18%). Methyl carbons at C(2) and C(6) and all H atoms are omitted.

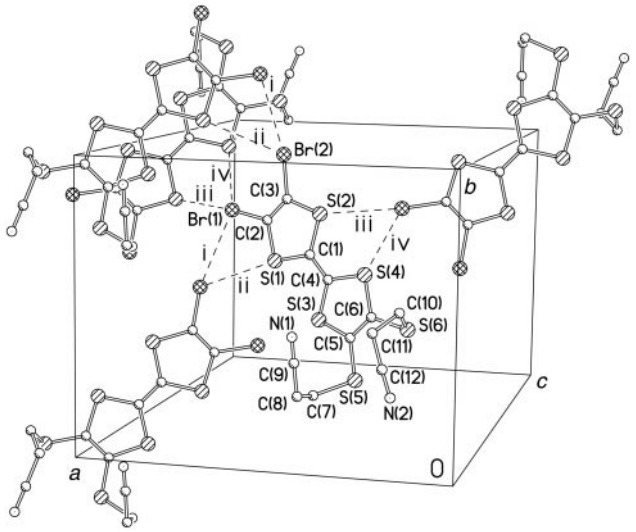

Fig. 6 Crystal structure of **15**, showing intermolecular contacts: Br···Br (i) 3.57; Br···S (ii) 3.68, (iii) 3.55, (iv) 3.74 Å. H atoms are omitted.

than the respective S(1)–C(2), S(2)–C(3) and C(2)–C(3) bonds in the Br-substituted ring (1.754(2), 1.754(2) and 1.331(2) Å respectively). The 'inner' C–S bonds differ only marginally, averaging 1.769(2) Å in the S-substituted and 1.762(2) Å in the Br-substituted ring. No continuous stacks exist in the structure; molecules pack in face-to-face pairs (pseudo-dimers) with an interplanar separation of 3.5 Å and a lateral slip between the molecules. Molecules are linked by type *ii* contacts Br(1)···Br(2) of 3.57 Å (*cf.* $D_i = 3.70$–3.94 Å, $D_a = 3.55$ Å) and Br(1)···S(2) of 3.55 Å ($D_i = 3.67$–3.81 Å, $D_a = 3.55$ Å); the interactions Br(1)···S(2) 3.74 Å and Br(2)···S(1) 3.68 Å are somewhat weaker.

Complexes 3·TCNQ, 4·TCNQ, 1·18, and salts $5^{+}\cdot I_3^{-}\cdot\frac{1}{2}I_2$ and $16^{+}\cdot I_3^{-}$. Structures **3**·TCNQ and **4**·TCNQ (Fig. 7) display a broadly similar packing motif comprising mixed stair-like stacks of alternating donor and acceptor molecules, with a longitudinal slip between adjacent molecules (Fig. 8). The interplanar separations of *ca.* 3.46 Å in **3**·TCNQ and 3.50 Å in **4**·TCNQ are typical for van der Waals interactions. This packing can be also described as a succession of infinite 2-dimensional layers. In both donor molecules the bis-SMe substituted dithiole ring is folded along the S(3)···S(4) vector by 9° (**3**) and 11° (**4**), while the iodo-substituted dithiole ring remains almost planar. The overall charge δ of a TCNQ molecule can be calculated from bond distances therein (Chart 2), using the linear dependence[37] $\delta = 4.18\ [0.476 - c/(b+d)]$, which gives $\delta = -0.2$ for **3**·TCNQ and -0.3 for **4**·TCNQ, *i.e.* a degree of charge transfer characteristic for mixed-stack semiconductors and consistent with the IR spectroscopic data (see above). The donor molecules in both structures are disordered by a 180° rotation around their long axes. Thus in **3**·TCNQ the iodine substituent is located at C(12) and C(13) with the probabilities of 54 and 46%, the methyl group making up the balance. In **4**·TCNQ the iodine substituent is located at C(12) or C(13) with the probabilities of 97% and 3%, respectively. The minor position necessitates rearrangements elsewhere in the structure, to avoid unreasonably short intermolecular contacts, but such disorder of light atoms is beyond the sensitivity of the X-ray method. In **3**·TCNQ either position of the disordered iodine atom has one

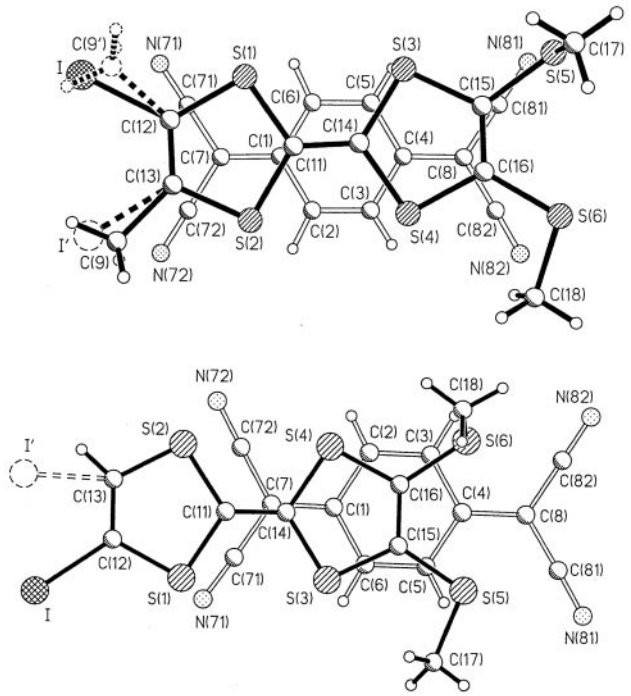

Fig. 7 Molecular overlap in the structures of **3**·TCNQ (top) and **4**·TCNQ (bottom).

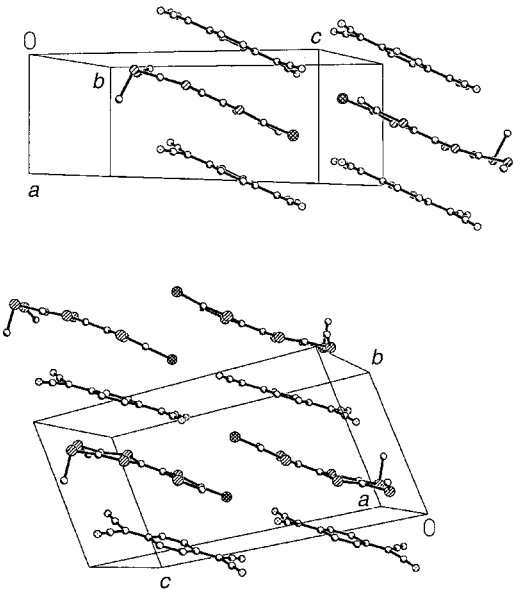

Fig. 8 Crystal packing in the structures of **3**·TCNQ (top) and **4**·TCNQ (bottom). H atoms are omitted.

short (inter-stack, but intra-layer) contact with a cyano group, with I···N distances of 3.14 and 3.18 Å (*cf.* $D_i = 3.58$–3.67 Å; $D_a = 3.42$ Å for C–I···N angles of 166 and 154°). In **4**·TCNQ a similar I···N contact is much longer (3.35 Å).

The structures of **1·18** and **1·19**·$2C_4H_8O_2$ also contain mixed stacks, the latter with dioxane molecules in inter-stack channels. The **18** moiety in **1·18** is disordered, one nitro-group being distributed between positions 4 [N(4), O(3A), O(4A)] and 5 [N(5), O(3B), O(4B)] with occupancies 74 and 26%, respectively. The collateral disorder of **1** was not satisfactorily resolved, which, together with the generally poor crystal quality (itself probably due to the disorder) resulted in low precision of the structure determination ($R = 0.13$).

The asymmetric unit of $\mathbf{5}^{+}\cdot I_3^{-}\cdot\frac{1}{2}I_2$ (Fig. 9) comprises one formula unit with the iodine molecule located at an inversion centre. Bond distances in the cation radical [central C=C 1.40(2), peripheral C=C 1.37(2), C–S average 1.72(2) Å] are normal for a +1 charged TTF system.[36] Two cation radicals form a dimer: the TTF moieties deviate from a perfectly eclipsed position by a lateral slip of 0.45 Å, their central C_2S_4 planes are separated by 3.35 Å and peripheral fragments tilt outwards of the dimer through a boat-like folding along the

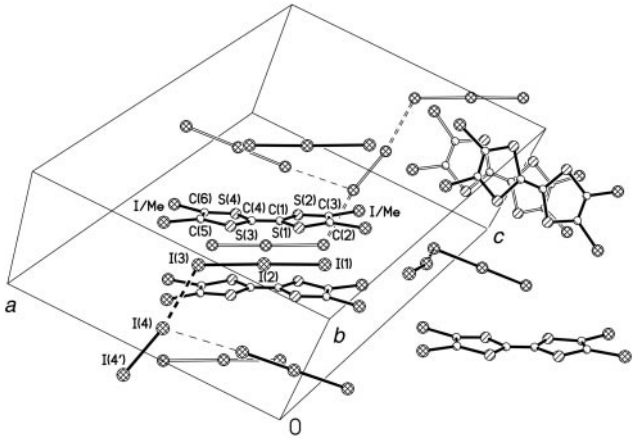

Fig. 9 Crystal structure of $\mathbf{5}^{+}\cdot I_3^{-}\cdot\frac{1}{2}I_2$, showing the I/Me superpositions as single atoms. Selected bond distances (Å) and angles (°): I(1)–I(2) 2.829(2), I(2)–I(3) 3.047(2), I(3)···I(4) 3.377(2), I(4)–I(4′) 2.788(3), I(1)–I(2)–I(3) 178.92(5), I(2)–I(3)–I(4) 118.83(5), I(3)–I(4)–I(4′) 169.04(7). I(4) and I(4′) are related *via* an inversion centre.

S···S vectors by 4° and 6°. The shortness of inter-cation contacts within the dimer (S···S 3.38–3.39 Å, C···C 3.35 Å) is consistent with electron coupling. There are no continuous stacks, every cation pair is surrounded by four I_3^- anions, parallel to within 1° of the cation's long axis. The resulting I···S distances (3.88–3.97 Å) correspond to normal van der Waals contacts ($D_i = 3.84$–3.97 Å). The cation is disordered: the iodine substituent is distributed between all four positions with occupancies estimated as 25, 25, 35 and 15%, methyl groups making up the balance. Two of these iodine positions, I(12) and I(16), approach I(4) of the iodine molecule at short distances of 3.46 and 3.88 Å (*cf.* $D_a = 4.00$ and 4.13 Å, respectively) suggestive of bonding interactions. Secondary bonds I(3)···I(4) [3.377(2) Å] also join the I_2 molecule and two anions into an I_8^{2-} unit, the strength of these interactions is confirmed by non-equivalence of I–I bonds within the anion, *viz.* I(1)–I(2) 2.829(2) Å and I(2)–I(3) 3.047(2) Å (*cf.* 2.907–2.927 in a standard isolated I_3^- anion).

The motif of planar organic cations sandwiched between anionic polyiodide chains has been observed before in the structures of several polyiodide salts of tetramethylpyrazinium, acridinium, 9-methyl- and 9-iodomethylacridinium.[38] The latter structure, like that of $\mathbf{5}^{+\cdot}I_3^-\cdot\frac{1}{2}I_2$, is stabilised by C–I···I_3^- interactions. However, the cations in these structures aquire positive charge through protonation of a heterocyclic N atom, rather than through a proper CT process, while genuine CT ($n\rightarrow\sigma^*$) complexes of iodine with dipyridylquinoxaline, 4-cyanopyridine, 4,4′-bipyridine, quinoxaline and tetramethylpyrazine,[39] contain no polyiodide chains, only I_2 molecules linked to nitrogen atoms by weak donor–acceptor N···I bonds of 2.40–2.95 Å. Pennington *et al.* have commented that polyiodide salts with more than three iodine atoms per organic cation are rare,[38b] although we note that salts of organosulfur electron donors seem to be unusual in this regard with a value of 4 : 1 in the present compound (*i.e.* $\mathbf{5}^{+\cdot}I_3^-\cdot\frac{1}{2}I_2$) and even higher ratios (7 : 1 and 8 : 1) being observed in other cases with derivatives of 1,4-dithiine and TTF as the cation moieties.[40]

The crystal structure of $\mathbf{16}^{+\cdot}I_3^-$ at 120 K (Fig. 10) is essentially the same as that found earlier at room temperature.[8d] Systematic differences in bond lengths (due to reduced librational shortening) are small, except for the C(1)=C(3) bond: 1.374(8) Å in the present work, *vs.* 1.42(1) Å in ref. 8*d*. Both the cation radical and anion species lie in the (100) mirror plane and possess crystallographic *mm*2 (C_{2v}) symmetry, the twofold axis passing through the C(1), C(3) and I(1) atoms. The structure thus comprises layers with interplanar separations of *a*/2, or 3.55 Å. Cations of one layer overlapping with anions of the next, the packing can also be described as mixed stacks parallel to the *a* axis, but this formal description does not account for the relatively high electrical conductivity of this salt (see above). However, $\mathbf{16}^{+\cdot}I_3^-$ shows two features necessary for an organic metal: *partial* charge transfer and a continuous system of short non-bonding contacts. Compared to neutral

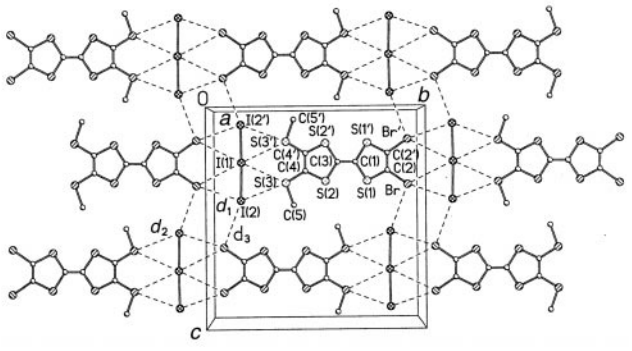

Fig. 10 Crystal structure of $\mathbf{16}^{+\cdot}I_3^-$. Symmetrically related atoms are primed. H atoms are omitted.

16,[8d] the C=C bonds in the TTF moiety of $\mathbf{16}^{+\cdot}I_3^-$ are longer and the C–S bonds shorter, as could be expected upon withdrawal of electrons (see above). The most reliable estimate of the positive charge on a TTF moiety can be made from the 'inner' C–S bond lengths. These bonds in $\mathbf{16}^{+\cdot}I_3^-$, C(1)–S(1) 1.738(3) Å and C(3)–S(2) 1.730(3) Å, are shorter than in the neutral **16** (1.756(4) and 1.763(4) Å, respectively) but still significantly longer than in $TTF^{+\cdot}$ cation radicals, *e.g.* 1.713(9) Å in $(TTF)(ClO_4)$[36c] and 1.718(4) in $(TTF)(SnMe_2Cl_3)$.[36d] The linear C–S distance–charge correlation[36b] gives a charge of $+\frac{2}{3}$ in $\mathbf{16}^{+\cdot}I_3^-$. The same value can be derived from the length of the central C(1)=C(3) bond, intermediate between 1.334(5) Å in **16** and 1.400 Å in $TTF^{+\cdot}$. On the other hand, the I(1)–I(2) bond, 2.900(3) Å, is shorter than usual for triiodide anions (2.907 to 2.927 Å, average 2.917 Å).[41] This can be explained by a partial electron withdrawal from the non-bonding HOMO, *i.e.* by a charge less than −1.

The anion in $\mathbf{16}^{+\cdot}I_3^-$ bridges the two adjacent cations along the *y* direction through short I···Br (d_1 in Fig. 10) and I···S (d_2) contacts with the terminal iodine atom I(2). The same I(2) atom forms a I···Br contact (d_3) in the *z* direction, resulting in a two-dimensional network within the layer. The d_1 and d_3 contacts are of type *ii*, favourable for I–Br and Br–I donation respectively. The d_1 distance of 3.604(1) is shorter than $D_a = 3.67$ Å; d_3 of 3.851(1) Å is longer than $D_a = 3.60$ Å, although both contacts are shorter than $D_i = 3.90$–4.11 Å. The d_2 contact of 3.719(1) Å is also shorter than $D_a = 3.84$–3.97 Å.

Conclusions

This study shows that the strategy of substituting TTF derivatives with iodine or bromine atoms leads to compounds which retain good π-electron donor characteristics and readily form crystalline charge transfer complexes and ion radical salts. X-Ray analyses reveal that they are prone to disorder, because of the similar sizes of methyl and iodo (or bromo) substituents. The iodo-substituents on a TTF moiety can participate in a variety of electrostatic and/or weak charge-transfer (donor–acceptor) interactions, bromo-substituents much less so. Although the exact nature of these interactions and their role in defining the packing motif is difficult to predict, it is clear that the halogens facilitate close intra- and inter-stack contacts, thereby enhancing dimensionality in the system, and providing a means of modifying the solid state properties. The availability of a wide range of halogenated TTF derivatives in synthetically useful amounts will enable further salts to be obtained and thereby enhance our understanding of the role that halogen substituents play in this class of materials.

Experimental

^1H and ^{13}C spectra were obtained on Varian Unity 300, Varian Mercury 200 and Varian VXR 400s spectrometers; chemical shifts are quoted in ppm, relative to tetramethylsilane (TMS) as an internal reference (0 ppm). Mass spectra were recorded on a Micromass Autospec spectrometer operating at 70 eV with the ionisation mode as indicated. Melting points were recorded on a Reichert-Kofler hot-stage microscope and are uncorrected. Infra-red spectra were recorded using a Paragon 1000 FTIR spectrometer operated from a Grams Analyst 1600; samples were embedded in KBr discs unless otherwise stated. Elemental analyses were obtained on a Carlo-Erba Strumentazione instrument. Cyclic voltammetric data were obtained on a BAS 50W electrochemical analyser (1×10^{-4} M solution of donor in acetonitrile under argon, 1×10^{-1} M tetrabutylammonium perchlorate supporting electrolyte, platinum working and counter electrodes, Ag/AgCl reference electrode, 20 °C).

SEEPR experiments were carried out in a flat quartz cell. The Pt gauze working electrode was inserted into the flat portion of the cell. The Ag wire pseudoreference electrode was positioned directly above the working electrode to reduce the *iR*-drop and the auxiliary electrode, a Pt wire spiral of large surface area, occupied the solvent reservoir above the flat section. EPR spectra were recorded on an IBM ESP-300 X-band spectrometer equipped with a TE_{104} dual cavity. Solutions of compounds **5–7** (10^{-3} M in CH_2Cl_2, 0.1 M $Bu_4N^+ClO_4^-$) were degassed by bubbling argon through them for 5 min and then injected into the SEEPR cell, which had previously been flushed with argon. Bulk electrolysis was then carried out simultaneously with signal acquisition (12.5 kHz field modulation, modulation amplitude 0.04 G, SEEPR spectrum centred at 3484.4 G and 20 G sweep width). Hyperfine coupling constants were obtained through spectral simulation and iterative curve fitting using the Winsym package.[42] Conductivity data were obtained using routine two- or four-probe methods.[43] Reactions were carried out under an argon atmosphere; reagents were of commercial quality and used as supplied unless otherwise stated; solvents were dried where necessary using standard procedures and distilled for chromatographic use. Column chromatography was performed on Prolabo silica (70–230 mesh).

Tetraiodotetrathiafulvalene 2

TTF (100 mg, 0.5 mmol) dissolved in tetrahydrofuran (14 cm^3) was cooled to −50 °C and lithium diisopropylamide–tetrahydrofuran complex (2.80 cm^3, 4.0 mmol of a 1.5 M solution in cyclohexane) was added. After stirring for 1 h, perfluorohexyl iodide (1.81 g, 4.0 mmol) was added in one portion. After a further 1 h at −50 °C, the cooling bath was removed and the reaction was left to warm to room temperature. The solvent was evaporated *in vacuo* and the residue was extracted with carbon disulfide. This extract was evaporated and the product crystallised from chlorobenzene to afford **2** (300 mg, 84%) as red needles, mp 203 °C (decomp.) [lit., 175 °C (decomp.);[13] 196–202 °C (decomp.)[14]] (Analysis found: C, 10.3; S, 18.4; $C_6I_4S_4$ requires: C, 10.2; S, 18.1%); *m/z* (EI) 708 (M^+, 100%), 582 ($M-I^+$, 50%), 456 ($M-2I^+$, 20%), 331 ($M-3I^+$, 5%).

4-Iodo-5-methyl-4′,5′-bis(methylsulfanyl)tetrathiafulvalene 3

A solution of 4-methyl-4′,5′-bis(methylsulfanyl)TTF[44] (600 mg, 1.93 mmol) in dry ether (75 cm^3) was cooled to −78 °C and LDA (1.5 M in cyclohexane, 1.4 cm^3, 2.15 mmol) was added dropwise over 2 min. The mixture was stirred at −78 °C for 3 h then perfluorohexyl iodide (0.83 cm^3, 3.8 mmol) was added and the reaction was allowed to reach 20 °C overnight. The mixture was concentrated *in vacuo* and the residue was dissolved in toluene, which was washed with water; the organic layer was then separated and dried ($MgSO_4$). Purification by column chromatography on silica gel (eluent hexane–toluene 5 : 1 v/v) followed by recrystallisation from dichloromethane–hexane gave **3** (550 mg, 65%) as red crystals, mp 89–90 °C (Analysis found: C, 25.0; H, 2.0; $C_9H_9IS_6$ requires: C, 24.8; H, 2.0%); *m/z* (CI) 437 (MH^+, 100%), 312 (60%), 195 (12%); δ_H ($CDCl_3$) 2.41 (6H, s), 2.07 (3H, s).

4-Iodo-4′,5′-bis(methylsulfanyl)tetrathiafulvalene 4

To a stirred solution of 4,5-bis(methylsulfanyl)tetrathiafulvalene[7b] (400 mg, 1.35 mmol) in dry diethyl ether (100 cm^3) at −78 °C under an atmosphere of argon was added lithium diisopropylamide (1.5 M in cyclohexane, 0.9 cm^3, 1.35 mmol) and stirring continued for 2 h. Perfluorohexyl iodide (1.5 cm^3, 6.9 mmol) was added, the mixture stirred a further 1 h at −78 °C and then allowed to warm to room temperature overnight. Workup as described for **3** and chromatography of the residue on a silica column (eluent hexane–toluene (1 : 4 v/v) afforded compound **4** as an orange solid (225 mg, 40%), mp 90 °C (Found: C, 22.6; H, 1.6%; $C_8H_7IS_6$ requires C, 22.7; H, 1.7%); *m/z* (DCI) 423 (MH^+, 100%), 297 (35), 195 (30); δ_H [$(CD_3)_2CO$] 6.91 (1H, s), 2.46 (6H, s). Continued elution afforded unchanged 4,5-bis(methylsulfanyl)tetrathiafulvalene (180 mg, 45%).

4-Bromo-4′,5,5′-trimethyltetrathiafulvalene 6

To a stirred solution of trimethyltetrathiafulvalene[21] (1.0 g, 4.06 mmol) in dry THF (100 cm^3) at −78 °C under an atmosphere of argon was added lithium diisopropylamide (1.5 M in cyclohexane, 2.98 cm^3, 4.46 mmol) and stirring continued for 2 h. 1,2-Dibromotetrafluoroethane (1.2 cm^3, 10.15 mmol) was added, the mixture stirred for a further 1 h at −78 °C and then allowed to warm to 20 °C overnight. Toluene (100 cm^3) was added and the mixture filtered through a 3 cm plug of silica eluting with toluene. After evaporation of the solvent, the residue was recrystallised twice from acetonitrile to afford compound **6** as orange–red crystals (1.21 g, 91%), mp 174–175 °C (decomp.) (Found: C, 33.4; H, 2.8%; $C_9H_9BrS_4$ requires C, 33.2; H, 2.8%); *m/z* (DCI) 324, 326 (MH^+, 100%), 247, (20), 131 (95); δ_H ($CDCl_3$) 2.01 (3H, s), 1.94 (6H, s).

4-Chloro-4′,5,5′-trimethyltetrathiafulvalene 7

Trimethyltetrathiafulvalene (1.0 g, 4.06 mmol) was lithiated as described above. Hexachloroethane (2.4 g, 10.15 mmol) was added, and workup as described for **6** gave a residue which was recrystallised three times from acetonitrile to afford compound **7** as orange–red crystals (741 mg, 65%), mp 196–197 °C (Found: C, 38.2; H, 3.2%; $C_9H_9ClS_4$ requires C, 38.5; H, 3.2%); *m/z* (DCI) 281, 283 (MH^+, 100%), 247, (25), 131 (90); δ_H ($CDCl_3$) 2.00 (3H, s), 1.94 (6H, s).

4-Bromo-1,3-dithiole-2-thione 13 and 4,5-dibromo-1,3-dithiole-2-thione 14

To a stirred solution of **12** (200 mg, 1.49 mmol) in diethyl ether (20 cm^3) at −78 °C was added lithium diisopropylamide–tetrahydrofuran complex (3.0 cm^3, 4.4 mmol of a 1.5 M solution in cyclohexane) over 15 min. After stirring at −78 °C for 3 h, a solution of toluene-*p*-sulfonyl bromide (1.06 g, 4.47 mmol) in ether (10 cm^3) was added and stirring continued for a further 3 h at −78 °C, and then the mixture was allowed to reach 20 °C overnight. The solvent was evaporated, the residue was extracted with dichloromethane, the organic extract was washed with water, separated, dried ($MgSO_4$) and evaporated to afford the crude product. Chromatography on a silica column (eluent hexane–toluene 4 : 1 v/v) afforded **14**, followed by **13**. Both products were recrystallised from hexane–toluene. Compound **13** (84 mg, 27%) yellow crystals, mp 92–95 °C (Analysis found: C, 17.3; H, 0.7; C_3HBrS_3 requires: C, 16.9; H, 0.5%); *m/z* (EI) 214 (M^+, 100%); δ_H (DMSO-d_6) 7.71 (s); δ_C (DMSO-d_6) 209.8, 129.2, 72.1. Compound **14** (120 mg, 30%) golden yellow crystals, mp 90–92 °C (Analysis found: C, 12.6; $C_3Br_2S_3$ requires: C, 12.3%); *m/z* (EI) 292 (M^+, 100%).

4,5-Dibromo-4′,5′-bis(2′-cyanoethylsulfanyl)tetrathiafulvalene 15

To a stirred solution of **14** (100 mg, 0.35 mmol) and **11**[17] (400 mg, 1.4 mmol) in toluene (25 cm^3) was added triethyl phosphite (0.35 cm^3, 2.0 mmol) and the mixture refluxed for 4.5 h. Removal of the solvent *in vacuo* gave a crude product which was purified by chromatography on a silica column, initially using hexane as the eluent to remove excess triethyl phosphite, followed by dichloromethane as eluent to give product **15** (69 mg, 38%) as yellow crystals, mp 132–134 °C (from acetonitrile) (Analysis found: C, 27.2; H, 1.7; N, 5.2; $C_{12}H_8Br_2N_2S_6$ requires: C, 27.1; H, 1.5; N, 5.3%); *m/z* (DCI)

536 ($M+1^+$, 100%), 456 ($M-Br^+$, 40%); δ_H ($CDCl_3$) 3.13 (4H, t, *J* 7 Hz), 2.79 (4H, t, *J* 7 Hz).

4,5-Dibromo-4′,5′-bis(methylsulfanyl)tetrathiafulvalene 16

To a stirred solution of **12** (118 mg, 0.22 mmol) in tetrahydrofuran (20 cm^3) at 20 °C was added a solution of caesium hydroxide hydrate (35 mg, 0.21 mmol) in methanol (5 cm^3) in one portion. Stirring was continued for 0.5 h, whereupon iodomethane (0.3 cm^3, excess) was added. The mixture was stirred at 20 °C for a further 2 h, then evaporated to leave a residue which was dissolved in dichloromethane and washed with water. The organic layer was separated, dried ($MgSO_4$) and evaporated to afford a crude product which was purified on a silica column (eluent hexane–dichloromethane 1 : 1 v/v) to yield **16** (75 mg, 75%) as orange crystals, mp 121–122 °C (lit.[8d] 121.5–122 °C) (Analysis found: C, 21.1; H, 1.3; $C_8H_6Br_2S_6$ requires: C, 21.2; H, 1.3%); *m/z* (EI) 454 (M^+, 100%); δ_H ($CDCl_3$) 2.47 (s).

Complex 2·F_4TCNQ

Solutions of compound **2** in dry carbon disulfide and F_4TCNQ in dichloromethane were mixed at 20 °C to afford tiny black crystals, σ_{rt} (compressed pellet measurement) = 0.2 S cm^{-1}.

Complex 3·TCNQ

Hot equimolar solutions of compound **3** and TCNQ (**17**) in dry acetonitrile were mixed and allowed to cool to 20 °C to afford long black needles of the complex **3**·TCNQ (stoichiometry determined by X-ray analysis); σ_{rt} (two probe measurement) = 2.0×10^{-9} S cm^{-1}; ν_{max} (KBr) 2206 cm^{-1}.

Complex 4·TCNQ

Hot equimolar solutions of compound **4** and **17** in dry acetonitrile were cooled to 20 °C and after slow partial evaporation of the solvent the blue–black crystals which formed were collected by filtration and washed sequentially with cold acetonitrile and diethyl ether to afford **4**·TCNQ (Found: C, 38.6; H, 1.7; N, 8.9%; $C_{20}H_{11}IN_4S_6$ requires C, 38.3; H, 1.8; N, 8.9%); σ_{rt} (two probe measurement) = 10^{-7} S cm^{-1}; ν_{max} (KBr) 2204 cm^{-1}.

Complex 1·18

4-IodoTTF **1**[10] (9.0 mg, 0.28 mmol) was dissolved in hot acetonitrile (2.0 cm^3) and 2,4,7-trinitro-9-dicyanomethylenefluorene **18** (9.7 mg; 0.27 mmol) was added. The mixture was stirred with heating to bring about complete dissolution. Chlorobenzene (0.7 cm^3) was then added and the mixture was allowed to cool slowly to 20 °C over a few days affording long needles of the complex **1·18** (Analysis found: C, 38.2; H, 1.2; N, 10.3; $C_{22}H_8IN_5O_6S_4$ requires: C, 38.1; H, 1.2; N, 10.1%); σ_{rt} (two probe measurement) = 10^{-8} S cm^{-1}.

Complex 1·19·($C_4H_8O_2$)$_2$

4-IodoTTF **1** (3.8 mg, 0.12 mmol) and 2,4,5,7-tetranitro-9-dicyanomethylenefluorene **19** (4.7 mg; 0.12 mmol) were dissolved in hot acetonitrile (2.0 cm^3) and the mixture was allowed to cool slowly to 20 °C over a few days affording long needles of the complex. These needles, which were unsuitable for X-ray analysis, were dissolved in hot dioxane (1.0 cm^3) and this solution was cooled to 20 °C over several days affording black crystals of the complex **1·19**·($C_4H_8O_2$)$_2$ suitable for X-ray analysis. To obtain a sample for elemental analysis, the procedure was scaled up five-fold {Analysis found: C, 39.1; H, 2.4; N, 9.3; $C_{30}H_{23}IN_6O_{12}S_4$ [*i.e.* **1·19**·($C_4H_8O_2$)$_2$] requires: C, 39.4; H, 2.5; N, 9.2%}.

Salts $5^{+\cdot}I_3^-\cdot I_2$

Iodine vapour was diffused into a solution of **5** (10 mg) dissolved in acetonitrile (20 cm^3) at 20 °C to afford after 4 days long black needles (stoichiometry determined by X-ray analysis); σ_{rt} (four probe measurement) = 10^{-6} S cm^{-1}.

Salt 16·I_3

Iodine vapour was diffused into a solution of **16** (10 mg) dissolved in acetonitrile (20 cm^3) at 20 °C to afford after 3 days **16**·I_3 as long shining black needles (11 mg) (Analysis found: C, 11.3; H, 0.6; $C_8H_6Br_2I_3S_6$ requires: C, 11.5; H, 0.7%); σ_{rt} (four probe measurement) = 8×10^{-2} S cm^{-1}.

X-Ray diffraction

The X-ray diffraction experiment for **2** was carried out on a Siemens 4-circle diffractometer ($2\theta/\omega$ scan mode), for other compounds on a SMART 3-circle diffractometer with a 1K CCD area detector, using graphite-monochromated Mo-Kα radiation ($\bar{\lambda}$ = 0.71073 Å) and a Cryostream (Oxford Cryosystems) open-flow N_2 gas cryostat. A combination of 4 sets of ω scans; each set at different ϕ and/or 2θ angles, nominally covered over a hemisphere of reciprocal space (for **3**·TCNQ and **4**·TCNQ, full sphere was covered by 5 sets). Reflection intensities were corrected for absorption by numerical integration based on crystal face indexing, for **4**·TCNQ followed by a semi-empirical correction based on comparison of Laue equivalents.[45] Crystals of **1·18** were very poor diffractors, thus the experiment was performed with graphite-monochromated Cu-Kα radiation ($\bar{\lambda}$ = 1.54178 Å) on a Rigaku AFC6S 4-circle diffractometer (ω scan mode). This, however, resulted in high absorption, the empirical correction of which (on ψ-scans of 3 reflections, using TEXSAN software[46]) was not entirely satisfactory. The structures were solved by a combination of Patterson and direct methods and refined by full-matrix least squares against F^2 of all data, using SHELXTL software.[47] Non-H atoms were refined in anisotropic approximation and H atoms in isotropic one, except in disordered groups, where minor positions of non-H atoms were refined in isotropic approximation and H atoms treated in riding model. Occupancies of disordered positions in **5**, **3**·TCNQ, **1·18** were refined by least squares, in **6**, **4**·TCNQ, $5^{+\cdot}I_3^-\cdot\frac{1}{2}I_2$ were fixed at iterationally optimised levels. The C(TTF)–C(Me) bond lengths in **5**, **6** and $5^{+\cdot}I_3^-\cdot\frac{1}{2}I_2$ were constrained to 1.50(1) Å, the C(TTF)–I bonds in **5** to 2.08(1) Å, other disordered atoms were refined freely. Crystal **5** was a racemic twin, the two enantiomeric components contributing 44(7)% and 56(7)%, respectively. Crystal data and other experimental details are listed in Tables 3 and 4.

Supplementary crystallographic data for **2**, **5**, **6**, **8**, **15**, **3**·TCNQ, **4**·TCNQ, **1·18**, **1·19**·2$C_4H_8O_2$, $5^{+\cdot}I_3^-\cdot I_2$ and $16^{+\cdot}I_3^-$ have been deposited at the Cambridge Crystallographic Data Centre. CCDC reference numbers 161754–161764. See http://www.rsc.org/suppdata/jm/b1/b101866n/ for crystallographic files in .cif or other format, and a table of intermolecular contacts for these compounds and a figure of the crystal structure of complex **1·18**.

Acknowledgements

We thank EPSRC for funding the work in Durham (A. C., D. E. J., A. J. M., C. L. W.), the Royal Society for funding exchange visits to Durham by I. F. P. and the Royal Society of Chemistry for an International Authors Grant (to I. F. P.). J. A. K. H. thanks the EPSRC for a Senior Research Fellowship. The work at Amherst was supported by National Science Foundation grant CHE 9905492.

Table 3 Crystal data: neutral donors

Compound	**2**	**5**	**6**	**8**	**15**
Formula	$C_6I_4S_4$	$C_9H_9IS_4$	$C_9H_9BrS_4$	$C_{10}H_{12}S_4$	$C_{12}H_8Br_2N_2S_6$
Formula weight	707.9	372.3	325.3	260.4	532.4
T/K	293	295	150	120	150
Symmetry	Triclinic	Monoclinic	Triclinic	Triclinic	Orthorhombic
Crystal size/mm	$0.4\times0.2\times0.2$	$0.3\times0.08\times0.02$	$0.25\times0.15\times0.04$	$0.5\times0.14\times0.07$	$0.4\times0.3\times0.25$
a/Å	4.190(1)	6.225(1)	6.033(2)	6.047(1)	14.609(4)
b/Å	11.746(2)	15.209(3)	6.830(1)	6.772(1)	11.607(4)
c/Å	14.294(3)	6.766(1)	7.862(4)	7.796(1)	21.020(5)
α/°	95.18(1)	90	107.70(2)	107.64(1)	90
β/°	91.92(1)	96.65(1)	103.17(1)	103.91(1)	90
γ/°	96.69(1)	90	95.81(1)	96.56(1)	90
U/Å^3	695.2(3)	636.3(2)	295.4(2)	289.3(1)	3564(2)
Space group	$P\bar{1}$ (# 2)	$P2_1$ (# 4)	$P\bar{1}$ (# 2)	$P\bar{1}$ (# 2)	*Pbca* (# 61)
Z	2	2	1	1	8
D_x/g cm^{-3}	3.382	1.943	1.829	1.495	1.984
μ/mm^{-1}	9.53	3.13	4.14	0.78	5.25
Refls. total	3149	5227	2415	3566	27012
Max. 2θ/°	60	60	58	58	61
Refls. unique	2630	3068	1481	1512	5086
R_{int}	0.022	0.072	0.045	0.038	0.057
Transmission	0.115–0.252	0.407–0.926	0.478–0.854	0.697–0.948	0.176–0.366
Refls. $I\geqslant2\sigma(I)$	2377	2217	1223	1366	4324
R, $I\geqslant2\sigma(I$	0.054	0.078	0.056	0.025	0.029
$wR(F^2)$	0.153	0.221	0.156	0.066	0.066

Table 4 Crystal data: complexes and salts

Compound	**3**·TCNQ	**4**·TCNQ	$\mathbf{5}^{+\bullet}I_3^-\cdot\frac{1}{2}I_2$	$\mathbf{16}^{+\bullet}I_3^-$	**1**·**18**	**1**·**19**·2dioxane
Formula	$C_9H_9IS_6\cdot C_{12}H_4N_4$	$C_8H_7IS_6\cdot C_{12}H_4N_4$	$C_9H_9IS_6{}^+I_3{}^-\cdot\frac{1}{2}I_2$	$C_8H_6Br_2S_6{}^+I_3{}^-$	$C_6H_3IS_4\cdot C_{16}H_5N_5O_6$	$C_6H_3IS_4\cdot C_{16}H_4N_6O_8\cdot 2C_4H_8O_2$
Formula weight	640.6	626.6	879.9	835.0	693.5	914.7
T/K	150	295	150	150	150	150
Symmetry	Triclinic	Triclinic	Monoclinic	Orthorhombic	Monoclinic	Monoclinic
Crystal size/mm	$0.4\times0.16\times0.13$	$0.3\times0.2\times0.1$	$0.44\times0.17\times0.008$	$0.3\times0.3\times0.04$	$0.3\times0.25\times0.01$	$0.4\times0.14\times0.07$
a/Å	7.635(1)	7.969(1)	14.034(11)	7.098(1)	11.209(4)	10.178(1)
b/Å	7.959(2)	9.066(1)	8.077(4)	16.255(1)	7.160(3)	24.490(1)
c/Å	20.021(3)	17.482(1)	17.960(4)	16.541(1)	29.917(3)	14.101(1)
α/°	81.20(1)	81.02(1)	90	90	90	90
β/°	88.64(1)	83.25(1)	107.20(1)	90	94.03(2)	100.99(1)
γ/°	87.21(1)	77.12(1)	90	90	90	90
U/Å^3	1200.7(3)	1211.7(2)	1945(2)	1908.5(3)	2394.9(13)	3450.3(4)
Space group	$P\bar{1}$ (#2)	$P\bar{1}$ (#2)	$P2_1/n$ (#14)	*Cmcm* (#63)	$P2_1/c$ (#14)	$P2_1/c$ (#14)
Z	2	2	4	4	4	4
D_x/g cm^{-3}	1.772	1.717	3.005	2.906	1.923	1.761
μ/mm^{-1}	1.87	1.86	8.41	9.74	14.24	1.24
Refls. total	13517	14342	13637	9133	4070	27818
Max. 2θ/°	60.3	61	55	61	120	61
Refls. unique	6362	6455	4308	1504	2913	9447
R_{int}	0.028	0.036	0.152	0.056	0.108	0.034
Transmission	0.593–0.810	0.345–0.933	0.124–0.933	0.093–0.678	0.382–1.000	0.677–0.919
Refls. $I\geqslant2\sigma(I)$	5505	4372	3068	1345	2120	7789
R, $I\geqslant2\sigma(I)$	0.041	0.041	0.077	0.025	0.130	0.034
$wR(F^2)$	0.092	0.094	0.224	0.061	0.338	0.076

References

1 Reviews and Monographs: (*a*) J. R. Ferraro and J. M. Williams, *Introduction to Synthetic Electrical Conductors*, Academic Press, London, 1987; (*b*) M. R. Bryce, *Chem. Soc. Rev.*, 1991, **20**, 355; (*c*) M. R. Bryce, *J. Mater. Chem.*, 1995, **5**, 1481; (*d*) P. Batail, K. Boubekeur, M. Fourmigué and J.-C. P. Gabriel, *Chem. Mater.*, 1998, **10**, 3005; (*e*) J. Yamada, H. Nishikawa and K. Kikuchi, *J. Mater. Chem.*, 1999, **9**, 617; (*f*) G. Saito in *Organic Molecular Solids: Properties and Applications*, ed. W. Jones, CRC Press, Boca Raton, 1997, Ch. 10, p. 309; (*g*) M. R. Bryce, *J. Mater. Chem.*, 2000, **10**, 589.

2 (*a*) G. R. Desiraju, *Crystal Engineering: The Design of Organic Solids*, Elsevier, Amsterdam, 1989; (*b*) R. Desiraju, *Chem. Commun.*, 1997, 1475.

3 *Supramolecular Engineering of Synthetic Metallic Materials: Conductors and Magnets*, eds. J. Veciana, C. Rovira and D. B. Amabilino, NATO ASI Series, Vol. 518, Kluwer, Dordrecht, 1999.

4 (*a*) F. Wudl, D. Wobschall and E. F. Hufnagel, *J. Am. Chem. Soc.*, 1972, **94**, 671; (*b*) J. Ferraris, D. O. Cowan, V. V. Walatka and J. H. Perlstein, *J. Am. Chem. Soc.*, 1972, **94**, 3372.

5 K. Deuchert and S. Hünig, *Angew. Chem., Int. Ed. Engl.*, 1978, **17**, 875.

6 (*a*) K. Bechgaard in *Structure and Properties of Molecular Crystals*, ed. M. Pierrot, Elsevier, Amsterdam, 1990, p. 235; (*b*) S. Roth, *One-Dimensional Metals*, VCH, Weinheim, 1995.

7 (*a*) A. S. Batsanov, M. R. Bryce, G. Cooke, J. N. Heaton and J. A. K. Howard, *J. Chem. Soc., Chem. Commun.*, 1993, 1701; (*b*) A. J. Moore, M. R. Bryce, A. S. Batsanov, J. N. Heaton, C. W. Lehmann, J. A. K. Howard, N. Robertson, A. E. Underhill and I. F. Perepichka, *J. Mater. Chem.*, 1998, **8**, 1541; (*c*) K. Heuzé, M. Fourmigué and P. Batail, *J. Mater. Chem.*, 1999, **9**, 2373; (*d*) J.-P. Legros, F. Dahan, L. Binet, C. Carcel and J.-M. Fabre, *J. Mater. Chem.*, 2000, **10**, 2685; (*e*) H. Li, D. Zhang, B. Zhang, Y. Yao, W. Xi, D. Zhu and Z. Wang, *J. Mater. Chem.*, 2000, **10**, 2063.

8 (*a*) C. Wang, J. Y. Becker, J. Bernstein, A. Ellern and V. Khodorkovsky, *J. Mater. Chem.*, 1995, **5**, 1559, and references therein; (*b*) T. Imakubo, H. Sawa and R. Kato, *Synth. Met.*,

1995, **73**, 117; (*c*) T. Imakubo, H. Sawa and R. Kato, *Synth. Met.*, 1997, **86**, 1847; (*d*) M. Iyoda, Y. Kuwatani, K. Hara, E. Ogura, H. Suzuki, H. Ito and T. Mori, *Chem. Lett.*, 1997, 599; (*e*) M. R. Bryce, A. J. Moore, A. S. Batsanov, A. Chesney, C. L. Wood and J. A. K. Howard, *Electrical, Optical and Magnetic Properties of Organic Solid State Materials IV*, eds. J. R. Reynolds, A. K.-Y. Jen, M. F. Rubner, L. Y. Chiang, and L. R. Dalton, Materials Research Society, Warrendale, Pennsylvania, 1998, **488**, 483; (*f*) T. Imakubo, T. Maruyama, H. Sawa and K. Kobayashi, *Chem. Commun.*, 1998, 2021.

9 (*a*) M. Jørgensen and K. Bechgaard, *Synthesis*, 1989, 207; (*b*) M. R. Bryce and G. Cooke, *Synthesis*, 1991, 263; (*c*) C. Wang, A. Ellern, V. Khodorkovsky, J. Bernstein and J. Y. Becker, *J. Chem. Soc., Chem. Commun.*, 1994, 983.

10 A. S. Batsanov, A. J. Moore, N. Robertson, A. Green, M. R. Bryce, J. A. K. Howard and A. E. Underhill, *J. Mater. Chem.*, 1997, **7**, 387.

11 (*a*) D. C. Green, *J. Org. Chem.*, 1979, **44**, 1476; (*b*) Review: J. Garín *Adv. Heterocycl. Chem.*, 1995, **62,** 249.

12 (*a*) R. D. McCullough, M. A. Petruska and J. A. Belot, *Tetrahedron*, 1999, **55**, 9979; (*b*) Reviews: M. Narita and C. U. Pittman, *Synthesis*, 1976, 489; (*c*) A. Krief, *Tetrahedron*, 1986, **42**, 1209; (*d*) G. C. Papavassiliou, A. Terzis and P. Delhaès, in *Handbook of Conductive Molecules and Polymers*, Vol. 1, ed. H. S. Nalwa, J. Wiley and Sons, Chichester 1997, 152.

13 R. Gompper, J. Hock, K. Polborn, E. Dormann and H. Winter, *Adv. Mater.*, 1995, **7**, 41.

14 M. Sato and M. Sensui, *J. Organomet. Chem.*, 1997, **538**, 1.

15 T. Shimizu, T. Koizumi, I. Yamaguchi, K. Osakada and T. Yamamoto, *Synthesis*, 1998, 259.

16 T. Imakubo, H. Sawa and R. Kato, *Synth. Met.*, 1997, **86**, 1883.

17 N. Svenstrup and J. Becher, *Synthesis*, 1995, 215.

18 R. Andreu, M. J. Blesa, J. Garín, A. López, J. Orduna and M. Savirón, *Synth. Met.*, 1997, **86**, 1897.

19 D. E. John, A. J. Moore, M. R. Bryce, A. S. Batsanov and J. A. K. Howard, *Synthesis*, 1998, 826. See also: D. E. John, A. J. Moore, M. R. Bryce, A. S. Batsanov, M. A. Leech and J. A. K. Howard, *J. Mater. Chem.*, 2000, **10**, 1273.

20 (*a*) J. Becher, J. Lau, P. Leriche, P. Mørk and N. Svenstrup, *J. Chem. Soc., Chem. Commun.*, 1994, 2715; (*b*) D. Damgaard, M. B. Nielsen, J. Lau, K. B. Jensen, R. Zubarev, E. Levellain and J. Becher, *J. Mater. Chem.*, 2000, **10**, 2249.

21 A. J. Moore, M. R. Bryce, A. S. Batsanov, J. C. Cole and J. A. K. Howard, *Synthesis*, 1995, 675.

22 (*a*) A. J. Moore and M. R. Bryce, *J. Chem. Soc., Chem. Commun.*, 1991, 1639; (*b*) D. L. Lichtenberger, R. L. Johnston, K. Hinkelmann, T. Suzuki and F. Wudl, *J. Am. Chem. Soc.*, 1990, **112**, 3302; (*c*) V. Khodorkovsky, A. Edzifna and O. Neilands, *J. Mol. Electron.*, 1989, **5**, 33; (*d*) V. Khodorkovsky and J. Y. Becker, in *Organic Conductors: Fundamentals and Applications*, ed. J. P. Farges, Marcel Dekker, New York, 1994, p. 75.

23 P. B. Ayscough, *Electron Spin Resonance in Chemistry*, Methuen and Co., London, 1967, pp. 20 and 27.

24 J. S. Chappel, A. N. Bloch, W. A. Bryden, M. Maxfield, T. O. Poehler and D. O. Cowan, *J. Am. Chem. Soc.*, 1981, **103**, 2442.

25 H. A. Bent, *Chem. Rev.*, 1968, **68**, 587.

26 F. H. Allen and O. Kennard, *Chem. Des. Autom. News*, 1993, **8**, 31.

27 A. S. Batsanov and J. A. K. Howard, *Acta Crystallogr., Sect. C*, 2000, **56**, 252; following the old low-precision study, R. H. Baughman, *J. Org. Chem.*, 1964, **29**, 964.

28 P. L. Southwick and J. R. Kirchner, *J. Org. Chem.*, 1962, **27**, 3305.

29 (*a*) V. R. Pedireddi, D. S. Reddy, B. S. Goud, D. C. Craig, A. D. Rae and G. R. Desiraju, *J. Chem. Soc., Perkin Trans. 2*, 1994, 2353; (*b*) G. R. Desiraju and R. Parthasarathy, *J. Am. Chem. Soc.*, 1989, **111**, 8725; (*c*) S. J. Harris, S. E. Novik, J. S. Winn and W. Klemperer, *J. Chem. Phys.*, 1974, **61**, 3866.

30 Yu. V. Zefirov and P. M. Zorkii, *Russ. Chem. Rev.*, 1995, **64**, 415.

31 R. S. Rowland and R. Taylor, *J. Phys. Chem.*, 1996, **100**, 7384.

32 A. Bondi, *J. Phys. Chem.*, 1964, **68**, 441.

33 S. C. Nyburg and C. H. Faerman, *Acta Crystallogr., Sect. B*, 1985, **41**, 274.

34 J. K. Badenhoop and F. Weinhold, *J. Chem. Phys.*, 1997, **107**, 5422.

35 I. Csöregh, E. Weber, T. Hens and M. Czugler, *J. Chem. Soc., Perkin Trans. 2*, 1996, 2733.

36 (*a*) L.-K. Chou, M. A. Quijada, M. B. Clevenger, G. F. de Oliveira, K. A. Abboud, D. B. Tanner and D. R. Talham, *Chem. Mater.*, 1995, **7**, 530; (*b*) D. A. Clemente and A. Marzotto, *J. Mater. Chem.*, 1996, **6**, 941; (*c*) K. Yakushi, S. Nishimura, T. Sugano and H. Kuroda, *Acta Crystallogr., Sect. B*, 1980, **36**, 358; (*d*) G. Matsubayashi, K. Ueyama and T. Tanaka, *J. Chem. Soc., Dalton Trans.*, 1985, 465; (*e*) T. Akutagawa, Y. Abe, T. Hasegawa, T. Nakamura, T. Inabe, K. Sugiura, Y. Sakata, C. A. Christensen, J. Lau and J. Becher, *J. Mater. Chem.*, 1999, **9**, 2737.

37 T. J. Kistenmacher, T. J. Emge, A. N. Bloch and D. O. Cowan, *Acta Crystallogr., Sect. B*, 1982, **38**, 1193.

38 (*a*) R. D. Bailey and W. T. Pennington, *Acta Crystallogr., Sect. B*, 1995, **51**, 810; (*b*) E. L. Rimmer, R. D. Bailey and W. T. Pennington, *J. Chem. Soc., Perkin Trans. 2*, 1998, 2557.

39 (*a*) R. D. Bailey, G. W. Drake, M. Grabarczyk, T. W. Hanks, L. L. Hook and W. T. Pennington, *J. Chem. Soc., Perkin Trans. 2*, 1997, 2773; (*b*) R. D. Bailey, M. Grabarczyk, T. W. Hanks and W. T. Pennington, *J. Chem. Soc., Perkin Trans. 2*, 1997, 2781; (*c*) R. D. Bailey, M. L. Buchanan and W. T. Pennington, *Acta Crystallogr., Sect. C*, 1992, **48**, 2259.

40 (*a*) M. R. Bryce, A. K. Lay, A. Chesney, A. S. Batsanov, J. A. K. Howard, U. Buser, F. Gerson and P. Merstetter, *J. Chem. Soc., Perkin Trans. 2*, 1999, 755; (*b*) A. S. Batsanov, D. E. John, M. R. Bryce and J. A. K. Howard, *Adv. Mater.*, 1998, **10**, 1360.

41 F. H. Allen, O. Kennard, D. G. Watson, L. Brammer, A. G. Orpen and R. Taylor, *J. Chem. Soc., Perkin Trans. 2*, 1987, S1.

42 NIEHS WinSym EPR, version 0.95, D. Duling, Laboratory of Molecular Biophysics, NIEHS, NIH, DHHS

43 (*a*) F. Wudl and M. R. Bryce, *J. Chem. Educ.*, 1990, **67**, 717; (*b*) L. B. Coleman, *Rev. Sci. Instrum.*, 1975, **46**, 1175.

44 M. Fourmigué, F. C. Krebs and J. Larsen, *Synthesis*, 1993, 509.

45 G. M. Sheldrick, *SADABS: Program for scaling and correction of area detector data*, University of Göttingen, Germany, 1998.

46 *TEXSAN: Single crystal structure analysis software, Version 5.1*, Molecular Structure Corporation, Woodlands, Texas, USA, 1989.

47 *SHELXTL, An integrated system for solving, refining and displaying crystal structures from diffraction data, Version 5.10*, Bruker Analytical X-ray Systems, Madison, Wisconsin, USA, 1997.